

ORIGINAL ARTICLE

Genomics of variation in nitrogen fixation activity in a population of the thermophilic cyanobacterium *Mastigocladus laminosus*

Patrick R Hutchins and Scott R Miller

Division of Biological Sciences, The University of Montana, Missoula, MT, USA

Variation in phenotypic traits that contribute to fitness influences a population's evolutionary response and its impact on ecosystem function following environmental change, yet its amount and nature are rarely known. Here, we investigated variation in nitrogen (N) fixation activity and its genetic basis for a random sample of laboratory strains of the cyanobacterium *Mastigocladus laminosus* from a N-limited, geothermally influenced stream in Yellowstone National Park. In a linear mixed-effects model, temperature and genetic differences among strains were the most important factors explaining variation in activity. Genome-wide analyses of genetic divergence between groups of strains that varied in N fixation activity revealed that few loci were strongly associated with these phenotypic differences. Notably, a single nonsynonymous polymorphism in the sulfate assimilation gene *apsK* explained >25% of the variation in activity at high temperature. We further identified a role for allelic variation of multiple terminal cytochrome oxidases for different aspects of N fixation. In addition, genomes of strains that fixed the most N overall contained a nonsense mutation in a histidine kinase gene that is expected to disrupt normal protein function and may result in transcriptional rewiring. This study illustrates how taking complementary approaches to link phenotype and genotype can inform our understanding of microbial population diversity.

The ISME Journal (2017) 11, 78–86; doi:10.1038/ismej.2016.105; published online 9 August 2016

Introduction

Microbial populations often exhibit extensive genetic diversity (Cadillo-Quiroz *et al.*, 2012; Shapiro *et al.*, 2012), and patterns of genome variation are consistent with the action of past or ongoing selection resulting from spatial and/or temporal heterogeneity in the environment (Rosen *et al.*, 2015). Recently, it has been proposed that much of this diversity may be maintained by negative frequency-dependent selection on gene content variation underlying ecological and social interactions, such as phage resistance and the sharing of public goods, respectively (Rodriguez-Valera *et al.*, 2009; Cordero and Polz, 2014). However, the nature and genetic basis of the functional variation within microbial populations, as well as the evolutionary mechanisms that maintain it, remain poorly understood in general.

Developing a better understanding of the extent of variation for fitness-related traits within populations is important for several reasons. As first pointed out

by Darwin, heritable variation within a population represents the raw material of evolution by natural selection. The amount of this variation can impact how populations respond to environmental change, because the rate at which beneficial mutations arise and subsequently attain high frequencies is slow compared with the rate at which populations can potentially adapt from pre-existing genetic variation (Barrett and Schluter, 2008). Genetic diversity within populations also has potential implications for ecosystem resilience in a changing environment (Hughes *et al.*, 1997; Luck *et al.*, 2003; Reusch *et al.*, 2005; Ehlers *et al.*, 2008).

The ability to obtain sufficient nitrogen (N) is an important fitness component for all cells, and many bacteria and archaea can fix N in the absence of a preferred source of this nutrient. At White Creek, an N-limited, geothermally influenced stream in the Lower Geyser Basin of Yellowstone National Park, a population of the multicellular cyanobacterium *Mastigocladus (Fischerella) laminosus* fixes N by developing heterocysts (Miller *et al.*, 2006), which are terminally differentiated cells that spatially separate the oxygen-sensitive N fixation process from photosynthetic oxygen produced by surrounding vegetative cells. N fixation has a complex genetic basis in heterocystous cyanobacteria (Kumar *et al.*, 2010), requiring genes that regulate and specify the

Correspondence: S Miller, Division of Biological Sciences, The University of Montana, 32 Campus Drive no. 4824, Missoula, MT 59812, USA.

E-mail: scott.miller@umontana.edu

Received 14 March 2016; revised 7 June 2016; accepted 14 June 2016; published online 9 August 2016

morphological and physiological changes that occur during the differentiation process, in addition to N fixation (*nif*) genes that are common to all diazotrophs. Estimates of the number of genes that are differentially regulated during heterocyst development range from ~500 in *Nostoc punctiforme* (Campbell *et al.*, 2007) to over 1000 in *Anabaena* PCC 7120 (Ehira *et al.*, 2003). Among these are 100–140 'Fox' genes that are required for N fixation in the presence of oxygen (Wolk, 2000), including those involved in the remodeling of the cell surface to form an envelope of glycolipid and polysaccharide layers that provides a passive gas diffusion barrier to limit the entry of oxygen (Nicolaisen *et al.*, 2009).

While much is known from model cyanobacteria regarding the genes required to develop a heterocyst and perform N fixation, we are ignorant of both the amount and the genetic basis of phenotypic variation for this important biogeochemical process in strains from natural bacterial populations. Here, we assay variation in N fixation activity for 22 *M. laminosus* strains isolated from along the White Creek thermal gradient of 39–54 °C mean annual temperature (Miller *et al.*, 2009). We next used existing genome sequence data available for most of these strains (Sano *et al.*, submitted) to identify genes associated with phenotypic differences among strains. Genetic exchange along White Creek is generally high throughout much of the *M. laminosus* genome (Wall *et al.*, 2014), and, consequently, we could take advantage of historic recombination events in the population to identify regions of the genome that exhibit unusually high levels of genetic differentiation between phenotypically divergent strains. These complementary approaches provide insights into the connection between genotype and phenotype for a complex fitness-related trait.

Materials and methods

Nitrogen and carbon fixation assays

Axenic *M. laminosus* strains were grown in 75 ml of nitrate-containing D mineral salts medium (Castenholz, 1988) at a maintenance temperature of 50 °C and a light intensity of $105 \pm 5 \mu\text{mol m}^{-2} \text{s}^{-1}$ with cool white fluorescent bulbs. The first digit in a strain's name indicates the White Creek sampling site from which it was isolated (with '1' representing the most downstream and '5' the most upstream sites; Miller *et al.*, 2009). Subsamples of growing cultures were transferred to flasks containing ND medium (D medium without the addition of combined N; Castenholz, 1988) to establish steady-state growth in the absence of combined N, as in Miller *et al.* (2006, 2009). After 2 weeks, cultures were split into six sublimes, with three each moved to 37 °C and 55 °C growth chambers, respectively. Sublines were maintained in ND medium with a 12/12 h light/dark cycle. Growing cells from each subline were assayed for N fixation, as described below. For each strain,

assays were performed two times using independent starting culture inocula.

Subsamples from each subline were homogenized with a tissue grinder and normalized to an OD_{750} of 0.05 ± 0.003 with a Beckman Coulter DU 530 spectrophotometer (Brea, CA, USA). For dilution series of growing cultures from two White Creek strains, we determined that optical density has the expected linear relationship with dry weight for 3 ml of *M. laminosus* cell suspensions that had been filtered onto a 0.45 μm pore size Millipore filter and dried for 48 h in a desiccation chamber (Pearson's correlation coefficient $R=0.98$, $P<0.001$; Supplementary Figure 1). Cultures were harvested at the beginning of the light cycle and then homogenized such that clumps were broken up but long chains containing vegetative cells and heterocysts remained intact. N fixation rates were estimated by ethylene production in acetylene reduction assays (Stewart *et al.*, 1967). Assays were carried out in 10 ml of ND medium in 20 ml crimp-sealed vials at a light intensity of $105 \pm 5 \mu\text{mol m}^{-2} \text{s}^{-1}$. Samples were incubated for 4 h following the addition of 5 ml of acetylene gas (generated by adding 5 g of calcium carbide to 100 ml of deionized H_2O) and terminated by aspirating as much sample headspace as possible (~15 ml) and injecting it into a pre-evacuated 5 ml crimp vial. Ethylene production was measured by flame-ionization detection gas chromatography with a Shimadzu GC-2014 (Kyoto, Japan). Ethylene production measurements were estimated using a standard curve, blank corrected against parallel incubation vials that contained only ND growth medium and normalized by sample optical density. Microscopic counts of heterocyst frequency were performed for a randomly selected subline at each temperature treatment.

Carbon fixation was concurrently estimated by ^{14}C -bicarbonate incorporation (Miller *et al.*, 1998). Briefly, incubations were initiated with the addition of 0.2 μCi of ^{14}C -bicarbonate to 3 ml aliquots of each subline, carried out for 1 h under the same conditions as for the acetylene reduction assays and then terminated by the addition of 200 μl of formalin. Samples with formalin added at the start of the incubation were included to correct for non-biological uptake of radioisotope. Each sample was filtered onto a 0.45 μm GN-6 membrane filter (PALL Life Sciences, Port Washington, NY, USA), rinsed first with 3% HCl to remove unincorporated radioisotope and then rinsed with deionized water. Filters were placed into 20 ml scintillation vials and ventilated in a fume hood for 1 h before adding 1.5 ml of EcoLite scintillation fluid (MP Biomedicals, Santa Ana, CA, USA). Samples were read by a Beckman LS6000SE scintillation counter (Brea, CA, USA) and normalized to sample OD as above.

Statistical analysis

Because of the crossed experimental design and the heteroskedastic nature of the data, a linear mixed-

effects model was used using the R 'lme4' package (Bates *et al.*, 2014) to analyze the factors that contribute to variation in N fixation. Fixed factors of the model included normalized carbon fixation rate, temperature, heterocyst frequency and all possible interactions. The random-effects structure was designed such that the model accounted for variation within incubations and among strains across the two temperature treatments. Other variables in the model were removed via backwards stepwise nested hypothesis testing using the F-test until the lowest Akaike information criterion score was obtained. A *post hoc* pseudo- R^2 for linear mixed models (Nakagawa and Schielzeth, 2013) was used to approximate the model fit and estimate the amount of variation explained by fixed factors and individual random effects.

Identification of candidate genes associated with phenotypic variation

M. laminosus strains were grouped into classes based on N fixation activity at each temperature treatment and for overall pooled performance. For each data set, strains in the upper quartile of mean normalized ethylene production were treated as the 'upper' class, and those below this benchmark were categorized as the 'lower' class. Genome data for *M. laminosus* strains used in the analysis were obtained previously (Sano *et al.*, submitted). Briefly, paired-end Illumina sequence data were acquired to $>100\times$ coverage for 20 White Creek strains randomly selected from the laboratory strain collection. The genome sequence data have been deposited in the NCBI Sequence Read Archive (GenBank accession no. SRP075623). Draft genomes were assembled *de novo* using Velvet (Zerbino and Birney, 2008), and genome contigs were autoannotated with the RAST server (<http://rast.nmpdr.org/>; Aziz *et al.*, 2008).

For each genome, protein-coding genes (CDS) were extracted from GenBank files with `extract_feature_seq.PLS` (bioperl.org) to create individual FASTA-formatted files for each CDS. Orthologous CDS from individual genomes were combined into single files using sequential local `blastn` queries of a non-redundant database of CDS from the population. This procedure was used to create separate FASTA-formatted files of each CDS for the total sample and for the individual phenotypic classes described above.

Custom Perl scripts (Supplementary Information) were next used to estimate nucleotide diversity π (i.e., the probability that two randomly selected sequences in a sample differ in nucleotide identity at a site) within phenotypic classes and for the total sample. Only full-length CDS were included, and loci with fewer than 10 sequences were excluded from the analysis. From these π estimates, both the relative amount of genetic differentiation (Φ_{ST} , the fraction of total nucleotide diversity between classes; Nei, 1982) and absolute genetic differentiation

between phenotypic classes (D_{XY} ; i.e., the numerator of Φ_{ST}) were estimated for each polymorphic CDS. In addition, we used PERL scripts to identify individual alleles at each locus and build contingency tables of allele counts for both phenotypic classes. These tables were used to test for a statistical association between allele frequencies at a locus and phenotype with Fisher's exact tests. This test was chosen owing to the small sample sizes involved and to avoid the assumption that the data conform to a χ distribution. Although necessitated by the labor-intensive nature of assaying N fixation, a consequence of the small sample sizes in the study is that we did not have the statistical power to accurately discriminate false positives for Fisher's tests. For select candidate genes that exhibited extreme genetic differentiation by one or more of the above approaches, we therefore used generalized linear models both to test the significance (with Bonferroni correction) of the association between allelic and phenotypic variation and to estimate the amount of observed phenotypic variation explained by the locus. In addition, to assess whether any flanking non-coding variation was linked to a candidate gene, sliding windows with a window length of 100 nt and a step size of 25 nt were estimated with DNASP version 5.10 (Librado and Rozas, 2009) for aligned genome contigs containing the candidate gene.

Expression of candidate genes

Transcription during growth under different N conditions was assessed by reverse transcription-PCR for five strains representing different alleles for candidate genes 167-28586 (histidine kinase (HK)) and 28-39736 (*apsK*). Strains were grown in semi-continuous batch cultures in D medium until ~ 5 ml of cell biomass had accumulated and then washed two times in ND medium before transfer to triplicate flasks containing 250 ml of either ND or D medium. Cultures were maintained at 37 °C with a 12/12 h light/dark cycle. Approximately 0.5 ml of cell mass was collected at 0.5 (T_0), 6, 12, 18, 24, 36 and 48 h after transfer for ND cultures and once for mid-growth phase cultures in D medium. All samples were immediately snap frozen in liquid nitrogen and stored at -80 °C. A Qiagen RNeasy Mini Extraction Kit (Hilden, Germany) was used to isolate RNA according to the manufacturer's instructions. RNA quantity and quality was checked on a NanoDrop spectrometer (Wilmington, DE, USA). We used reverse transcriptase-negative controls to confirm the absence of genomic DNA contamination of the isolated RNAs using the PCR cycling conditions described below. If needed, an additional DNase digestion was performed before cDNA synthesis. A Thermo Scientific Maxima First-Strand cDNA Synthesis Kit (Thermo Fisher Scientific, Waltham, MA, USA) for reverse transcription-PCR was used to construct first-strand cDNA according to the manufacturer's instructions. First-strand synthesis was accompanied by a

template-negative control. For *HK* gene 167-28586, an ~1 kbp cDNA was amplified by touchdown PCR on an MJR PTC-100 thermal cycler (MJ Research, Waltham, MA, USA) with primers 5'-GGAATCCACCAACTATGG-3' and 5'-CCAGGTGTAGAGTAGCAC-3'. An initial 3 min denaturation step at 94 °C was followed by 30 cycles of 1 min at 94 °C, 30 s at variable annealing temperatures, and 1 min at 72 °C. The initial annealing temperature was 54 °C and decreased every 10 cycles, reaching a final annealing temperature of 50 °C. For adenylyltransferase kinase gene 28-39736, a ~300 bp cDNA product was amplified with primers 5'-GAAAACATCCGTCGCATTGG-3' and 5'-TGATGTAACCGAGTTCTGCC-3'. An initial denaturation step at 94 °C for 3 min was followed by 30 cycles of 1 min at 94 °C, 30 s at 52 °C and 30 s at 72 °C. The presence of cDNA amplicons was assessed by agarose gel electrophoresis.

Evolutionary history of the *apsK* candidate

A neighbor-net splits network was inferred with Splittree (Huson and Bryant, 2006) using default settings for sequence data from White Creek and for orthologs of the APS kinase candidate 28-39736 from representative *M. laminosus* strains from throughout its range (GenBank accession nos KX267709–KX267733), including *Mastigocladus* (= *Fischerella*) strain PCC 7521 (Dagan *et al.*, 2013).

Results and discussion

Nitrogen fixation activity of White Creek *M. laminosus* strains

We assayed N fixation by the acetylene reduction method (Stewart *et al.*, 1967) for 22 laboratory strains randomly selected from our culture collection for the White Creek *M. laminosus* population to estimate the extent of phenotypic variation for this trait. Strains were assayed at 37 °C and 55 °C, temperatures that delimit the approximate bounds of the population range. N fixation is energetically expensive, with high reductant requirements, and fixed carbon provisioned by adjacent vegetative cells contributes both electrons and a portion of the ATP budget for the process (Kumar *et al.*, 2010). We therefore simultaneously estimated carbon fixation to test whether rates of N fixation and carbon fixation are correlated. We might expect a positive correlation, as has previously been reported for *Anabaena* sp. (Oh *et al.*, 1991). On the other hand, because enhanced carbon fixation implies increased photosynthetic oxygen generation, which can potentially inhibit nitrogenase, the relationship between the two might be more complicated. Finally, we estimated heterocyst frequencies to test whether strains with more heterocysts fix more N.

We observed considerable variation among strains in N fixation activity (i.e., ethylene production normalized to cell density; Figure 1). The final linear mixed model included two fixed factors (heterocyst

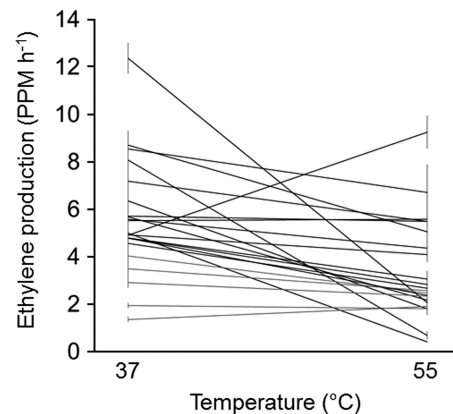


Figure 1 Ethylene production normalized by cell optical density among *M. laminosus* strains at 37 °C and 55 °C. Bars are s.e. Each trace represents a strain.

frequency and a carbon fixation \times temperature interaction) and two random effects (inoculum, i.e., assays of a strain derived from independent culture inocula, and a strain \times temperature interaction). The pseudo- R^2 for the model was 0.74, with random effects explaining 53% of the total variation. Of the random effects, strain identity and temperature explained comparable amounts of variation (19% and 20%, respectively), emphasizing the importance of both genetic differences among strains and the environment in determining activity. By contrast, the effect of inoculum was small (3%), indicating that a strain's activity was generally consistent between independent cultures.

With respect to the effects of temperature on N fixation, individual strains generally fixed more N at 37 °C than at 55 °C (Figure 1). This finding is corroborated by both $^{15}\text{N}_2$ -uptake experiments (Stewart, 1970) and acetylene reduction assays performed with *M. laminosus*-containing microbial mats from White Creek (Sano *et al.*, submitted). N fixation activity was significantly higher at the lower temperature for eight strains (*t*-tests, $P < 0.05$), and estimated activities for most other strains also tended to be higher at 37 °C. In only one case (strain WC344) was N fixation significantly greater at 55 °C.

Fixed factors explained roughly half as much variation as the random effects (21%). Average heterocyst frequency was $2.4 \pm 0.3\%$ (mean \pm 95% confidence interval). This is lower than the ~5–10% frequency typically reported for model heterocystous cyanobacteria (Kumar *et al.*, 2010) but comparable to previous observations for *M. laminosus* (unpublished data). A significant correlation between heterocyst frequency and N fixation was only observed at 55 °C (Pearson's correlation coefficient $R = 0.50$, $P < 0.01$) but was positive in sign for all data sets ($R = 0.17$ and 0.30 for the 37 °C and pooled data sets, respectively). Mean strain-specific normalized carbon fixation rates for the pooled data set ranged between 33 and $133 \mu\text{g C l}^{-1} \text{h}^{-1}$. In general, C and N

fixation activities are positively associated. The correlation between C and N fixation was significantly positive in the 55 °C ($R=0.73$, $P<0.01$) and pooled data sets ($R=0.59$, $P<0.01$), and positive, although not significant, at 37 °C ($R=0.50$, $P=0.25$).

Overview of genome-wide analyses of genetic variation associated with differences in N fixation activity

Differences among strains in N fixation activity accounted for more than one-quarter of the total variation explained by the model. We used annotated genome data that were available for 18 of the strains (Sano *et al.*, submitted) to identify the genes most strongly associated with these differences for the 37 °C, 55 °C and pooled data sets, respectively. To do so, we first binned strains into 'upper' (upper quartile of mean N fixation activity) and 'lower' phenotypic classes for each data set. Four of the six strains (WC114, WC119, WC1110 and WC245) in the upper quartile at 37 °C were isolated from lower temperature, downstream sites at White Creek, whereas four of the six strains (WC344, WC438, WC439 and WC542) in the upper quartile at 55 °C were isolated from higher temperature, upstream sites (Figure 1 and Supplementary Table 1). This observation is in accord with a general interaction between the temperature dependence of N fixation and the location along White Creek from which the strain was isolated ($F_{(1,24,4)}=4.1$; $P<0.05$). Specifically, although upstream (sites WC3–5) and downstream (sites WC1–2) strains did not significantly differ in N fixation at 37 °C (mean (s.e.) of 5.8 (0.45) versus 5.7 (0.32) p.p.m. ethylene produced per h for downstream and upstream strains, respectively), strains from the downstream sites exhibited lower rates of N fixation at 55 °C than did strains from upstream sites (3.5 (0.44) versus 5.0 (0.42) p.p.m. ethylene produced per h). This pattern is in agreement with our previous finding that upstream strains have much higher fitness at 55 °C than do downstream strains (Miller *et al.*, 2009). Still, there was considerable variation among strains with respect to the temperature dependence of N fixation and location along White Creek, which is of potential importance for ecosystem function given seasonal heterogeneity in temperature at different sites (Miller *et al.*, 2009). Among the strains in the upper quartile for the pooled data set, strains WC119, WC245 and WC439 were also in the upper quartiles for both temperature-specific data sets, whereas the other strains were in the upper quartile for one of the temperature treatments (Figure 1 and Supplementary Table 1).

We next estimated three measures of genetic differentiation between classes for each of the 2072 polymorphic protein-coding genes in the sample. We first used Fisher's exact test to evaluate whether allele frequencies at a locus were statistically different between classes. The second and third measures were both based on the amount of genetic

variation (nucleotide diversity, π) within and between phenotypic classes: Φ_{ST} is the fraction of the total variation that is between phenotypic classes, whereas D_{XY} is the average number of nucleotide differences per site between randomly selected sequences from different phenotypic classes. These metrics capture different aspects of divergence. For example, recently diverged alleles that contribute to phenotypic differentiation but differ by only one single-nucleotide polymorphism would be expected to be a candidate for the Φ_{ST} data set, whereas more divergent alleles would be expected to only be a D_{XY} candidate if they did not also exhibit an extreme difference in allele frequency between phenotypic classes.

For all three data sets, genetic differentiation between phenotypic classes was very low for the majority of the *M. laminosus* genome (i.e., Fisher's exact tests for allele frequency contingency tables were not significant and values of Φ_{ST} and D_{XY} were low; Supplementary Figures 2 and 3). Genes in the right tails of the respective frequency distributions represent the best candidates for loci that contribute to the observed genetic differences in N fixation activity among strains. Consequently, we focused on the loci exhibiting the most extreme differentiation between classes (Table 1). These included genes at a significance level of $P<0.01$ for a Fisher's exact test, a Φ_{ST} value >0.5 and a D_{XY} value >0.005 . For all three measures, these cutoffs represented $<0.3\%$ of polymorphic genes in any of the analyses.

There was little overlap among candidate loci for the three data sets (Table 1), which suggests that the genetic factors underlying variation between phenotypic classes largely differ for general N fixation performance (i.e., reflected in the pooled data set) as well as specific activities at the different temperatures. These apparent differences in genetic architecture make sense given that mean strain activities at 37 °C and 55 °C were not correlated overall ($P=0.43$). Similarly, only a minority of genes within each data set were candidates for multiple measures of genetic differentiation (Table 1). Below, we highlight a few particularly noteworthy candidates.

APS kinase at 55 °C

A 55 °C candidate with the greatest Φ_{ST} value and the most extreme differences in allele frequency between phenotypic classes of any analysis encodes the sulfate assimilation enzyme adenylylsulfate (APS) kinase (gene ID 28-39736; Table 1). The two alternative alleles at this locus differed by only a single nonsynonymous polymorphism, resulting in either an asparagine or an aspartate residue at codon 77, with the latter fixed (i.e., 100% frequency) in the upper class and the former at 83% frequency in the lower class. A sliding window analysis of the variation surrounding *apsK*, including flanking

Table 1 Genes associated with differences in N fixation activity between phenotypic classes of *M. laminosus* strains

Analysis	Annotation (gene ID)	P_{FET}	Φ_{ST}	D_{XY}
55 °C	Adenylsulfate kinase (28-39736)	0.0034	0.73	
	Hypothetical protein (26-13568)	0.0079		
	Glycosyltransferase (1-33964)		0.57	
	ATPase (49-34361)		0.53	
	CoxCI; Cyt oxidase subunit 3(65-42545)		0.52	
	Histidine kinase (93-42545)		0.52	
	ABC transporter (77-48944)			0.0081
UreA urease (10-32834)			0.0053	
37 °C	Riboflavin reductase (43-56937)	0.0082		
	Hypothetical protein (33-9029)			0.0057
Pooled	Histidine kinase (167-28586)		0.54	0.0161
	Glycine cleavage system (27-2489)	0.0057		
	CoxAII; Cyt oxidase subunit 1 (21-20552)	0.0070		
	ArsA ATPase (7-34642)	0.0070		
	Hypothetical protein (48-37089)	0.0083		
	Pleiotropic regulatory protein (84-29888)	0.0087		
	Cytochrome P450 (20-24813)		0.53	
	ABC transporter (77-48944)			0.0088
	Hypothetical protein (33-9029)		0.0057	
	UreA urease (10-32834)		0.0056	
	Hypothetical protein (93-17867)		0.0054	
Chlorophyll-binding protein (62-37089)		0.0052		

Abbreviation: P_{FET} , Fisher's exact test P -value.

regulatory DNA, which was invariant in the sample, confirmed that only this single-nucleotide polymorphism (SNP) is tightly associated with the differences between phenotypic classes (Figure 2a). The two SNP variants are not restricted to White Creek but, rather, are geographically widespread (Figure 2b), which suggests that the SNP is old and has been maintained by selection during *M. laminosus* diversification. This illustrates that functional variation observed within a population may pre-date earlier phylogenetic divergence. Such trans-specific polymorphisms are generally thought to be rare but may occur when spatiotemporal variation or other mechanisms of balancing selection actively maintain ancestral variation in the descendent lineages of a common ancestor over long evolutionary time scales (Hedrick, 2006). Both alleles are expressed during growth with combined N, during the heterocyst differentiation process, and during steady-state growth under N-fixing conditions (Supplementary Figure 4).

A longstanding question in evolutionary biology is whether functional differences within populations are primarily due to selection on variation for a few genes of major effect (e.g., >10% of the variation explained) or, alternatively, for many genes of small effect (Phillips, 2005). More than 25% of the variation in N fixation activity at 55 °C could be explained by which *apsK* allele a strain possessed ($R^2=0.28$; $P<10^{-6}$, significant after Bonferroni correction), indicating that this gene makes a major contribution to phenotypic variation. This contrasts with the 37 °C analysis, for which no strong candidate emerged (Table 1); in this case, a much larger sample size will be required to dissect the

genetic basis of variation in N fixation. Although the mechanism by which the different *apsK* alleles impact N fixation at 55 °C remains to be resolved, we note that the sulfur requirements for N fixation are high due to the demand for iron-sulfur clusters by nitrogenase (Rubio and Ludden, 2008).

Terminal cytochrome oxidases

Enhanced respiratory activity within a mature heterocyst by cytochrome oxidases both reduces oxygen concentration in the vicinity of nitrogenase and contributes ATP to N fixation. *Anabaena* PCC 7120 has three copies of the *coxBAC* operon (*coxBACI*, *coxBACII* and *coxBACIII*), and all are strongly upregulated following heterocyst maturation, with *coxBACII* and *coxBACIII* exhibiting particularly large expression changes compared with nitrate-grown cells (Flaherty *et al.*, 2011). The *M. laminosus* genome contains orthologs of all three operons, and components of each appear to be genetically differentiated between phenotypic classes for one or more of the analyses. For the allele frequency analyses, *coxAII* (gene ID 21-20552; Cyt *c* oxidase subunit 1) was the second-most differentiated gene for overall N fixation (Table 1), whereas *coxAIII* (gene ID 135-35450) was near our significance cutoff ($P=0.011$) for both the pooled and 37 °C analyses. At 55 °C, *coxCI* (gene ID 65-42545; Cyt *c* oxidase subunit 3) was a Φ_{ST} candidate. Given the importance of oxygen consumption for both ATP production and the maintenance of a microoxic environment in heterocysts, these results raise the possibility that this genetic variation may contribute

to N fixation differences among strains by impacting aerobic respiration activity, and these loci represent future targets for functional validation.

HK gene 167-28586

The most extreme outlier in both the Φ_{ST} and D_{XY} distributions for the pooled data set was an annotated *HK* gene (gene ID 167-28586; Table 1). Four percent of nucleotide sites were variable at this locus, 40 times greater than the genome-wide average (Sano *et al.*, submitted). Three alleles were identified: one

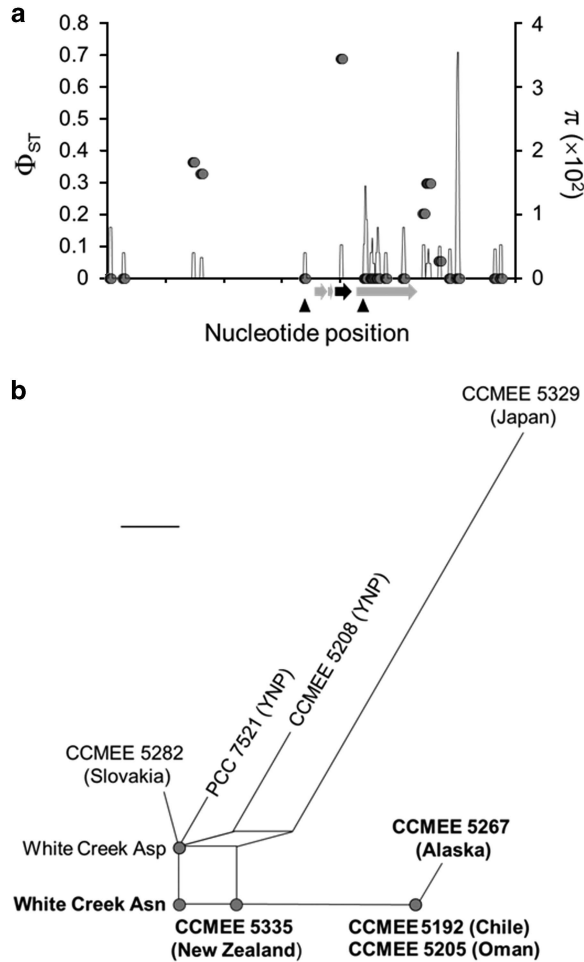


Figure 2 (a) Sliding window of genetic variation (nucleotide diversity π , line) and differentiation between phenotypic classes (Φ_{ST} , closed circles) for the 55 °C analysis for a ca. 14 kb region (axis ticks are 2 kb increments) surrounding the *apsK* candidate. The window length was 100 nt with a step size of 25 nt. SNPs flanking *apsK* (black arrow) are not associated with the phenotype (low Φ_{ST}) as a result of historic recombination events (closed triangles) that have broken up linkage between *apsK* and surrounding DNA. (b) Neighbor-net splits network of the evolutionary relationships among *apsK* alleles for *M. laminosus* strains from White Creek and throughout its global range. Because this history includes recombination, these relationships are better described by a network, which connects alleles related by recombination with cycles, than by a bifurcating tree. Nucleotide identity at position 229 is indicated, with A229 conferring the asparagine allele (bold) and G229 conferring the aspartate allele (normal font), respectively. Scale bar is 0.002 expected nucleotide substitutions per nucleotide site.

with a nonsense mutation 150 nucleotides upstream of the 3' end that was fixed in the upper class and at 36% frequency in the lower class; a full-length allele; and an apparently rare ($N=1$ in our sample) recombinant allele that is identical to the latter at the 5' end and to the former at the 3' end and therefore contains the nonsense mutation.

The comparatively high sequence divergence at this locus suggests either an idiosyncratically high evolutionary rate or that genetic variation has been maintained by some mechanism of balancing selection. The latter alternative is strongly supported by two molecular evolutionary signatures of long-term balancing selection observed for a random sample of 20 White Creek *M. laminosus* genomes (Figure 3a; Sano *et al.*, submitted). One is an extremely positively skewed value of Tajima's D (among the top 0.5% most positive values; Tajima, 1989), which indicates that the common ancestor of the alleles is older than expected under selective neutrality. The second is an excess of nucleotide polymorphism in the White Creek population compared with divergence from the sister taxon *Fischerella* PCC 7414, among the 2% highest values observed. This evidence for long-term balancing selection maintaining variation at this locus suggests that different alleles may be favored in different environments.

HKs participate in two-component signal-transduction systems, the principal means by which bacteria sense and respond to environmental changes (Gao and Stock, 2009). Following an environmental stimulus, the ATP-binding domain at the C-terminal end of an HK catalyzes the autophosphorylation of a conserved histidine

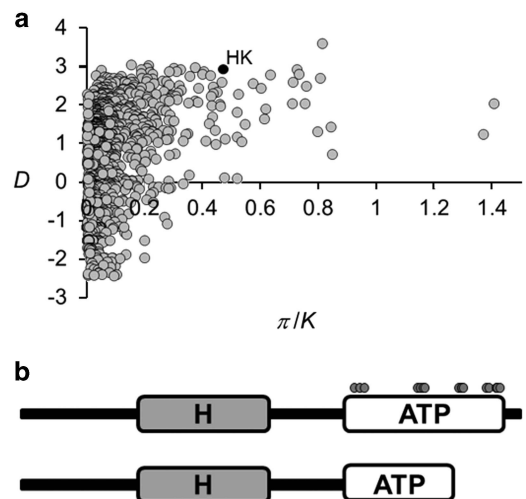


Figure 3 (a) *HK* candidate gene 167-28586 (HK, black circle) exhibits extreme values of both Tajima's D and the ratio of polymorphism (π) to divergence (K) from *Fischerella* strain PCC 7414 for 1623 orthologs that are polymorphic at White Creek. (b) Both the full-length (top) and nonsense (bottom) alleles of *HK* 167-28586 possess an intact H domain, but the nonsense mutation in the latter results in the loss of more than one-half of the ATP-binding residues (gray circles) in the binding pocket of the ATP domain.

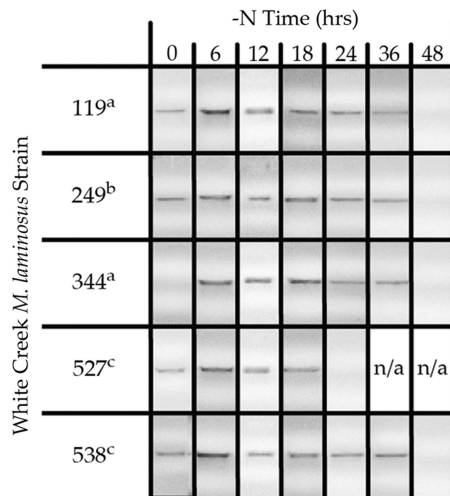


Figure 4 Presence or absence of an HK gene 167-28586 transcript after nitrogen step-down in five *M. laminosus* strains from White Creek. Subscripts indicate strain genotype ('a' is the nonsense allele, 'b' is the recombinant allele and 'c' is the full-length allele). With the exception of strain WC527, which had insufficient biomass after 24 h and was therefore not available for further analysis (N/A), the transcript could no longer be detected 48 h after the onset of N limitation.

residue. The HK then transfers the phosphoryl group to a cognate response regulator to effect a change in gene expression or protein activity (Galperin, 2010). The nonsense mutation in HK 167-28586 results in the loss of more than one-half of the ATP-binding pocket and of key ATP-binding residues (Figure 3b and Supplementary Figure 5), including the highly conserved G2 and G3 boxes required for autophosphorylation and kinase activities (Dutta and Inouye, 2000). This is expected to render this allele nonfunctional for these activities, with potential implications for the downstream regulation of gene expression. All three observed HK 167-28586 alleles were expressed during growth with nitrate (Supplementary Figure 6), immediately following N deprivation as well as during heterocyst development (Figure 4). However, because mature heterocysts were clearly visible at 36 h, the last time point for which the transcript was detected (Figure 4), we conclude that the gene is not expressed during steady-state growth under N-fixing conditions, following heterocyst differentiation. This suggests that any contribution of this locus to differences among strains in N fixation activity is a consequence of expression during the heterocyst development process itself, or, potentially, before the onset of N limitation.

Loss-of-function mutations that alter regulatory networks may be a common mechanism of bacterial adaptation to environmental change (Hottes *et al.*, 2013), and we speculate that the nonsense mutation in HK 167-28586 may result in transcriptional 'rewiring' that is somehow favorable with respect to N fixation. Resolution of this issue, however, will require characterization of its function, including the identification of its cognate response regulator(s) and the signal-transduction network in which it

participates. In addition, addressing whether there are fitness trade-offs in alternative environments (beyond N availability) among strains with different HK 167-28586 alleles will help to clarify the precise role that balancing selection has in the maintenance of variation at this locus.

Conclusion

Tests of genetic differentiation between phenotypic classes are a powerful way to identify the genetic variation that specifically contributes to functional differences among members of a population. Our results have revealed several candidate genes associated with differences in N fixation activity, some with clear links to heterocyst metabolism. In the case of *apsK*, we have resolved a single, geographically widespread SNP with a major effect on this ecologically important trait. Future efforts will be aimed at developing a conjugal transfer system for *M. laminosus* analogous to what has been recently accomplished for its close relative, *Fischerella muscicola* PCC 7414 (Stucken *et al.*, 2012). This will enable us to investigate the phenotypic effects of individual genetic variants (e.g., *apsK* and HK 167-28586 alleles) in an otherwise identical genetic background and thereby begin to develop a mechanistic understanding of their consequences for organism function.

Conflict of Interest

The authors declare no conflict of interest.

Acknowledgements

We thank the Cory Cleveland lab group for training and use of their gas chromatograph. Elizabeth Crone for statistical advice regarding the mixed-effects model and Kayli Anderson for assistance with the expression studies and DNA sequencing. We also thank two reviewers for their helpful comments and suggestions for improving the paper. This work was supported by US National Science Foundation award IOS-1110819 to SRM.

References

- Aziz RK, Bartels D, Best AA, DeJongh M, Disz T, Edwards RA *et al.* (2008). The RAST server: rapid annotations using subsystems technology. *BMC Genomics* **9**: 75.
- Barrett RD, Schluter D. (2008). Adaptation from standing genetic variation. *Trends Ecol Evol* **23**: 38–44.
- Bates D, Maechler M, Bolker B, Walker S. (2014). lme4: Linear mixed-effects models using Eigen and S4. R package version 1.0-6. Available at: <http://CRAN.R-project.org/package=lme4> (accessed 1 March 2014).
- Cadillo-Quiroz H, Didelot X, Held NL, Herrera A, Darling A, Reno ML *et al.* (2012). Patterns of gene flow

- define species of thermophilic Archaea. *PLoS Biol* **10**: e1001265.
- Campbell EL, Summers ML, Christman H, Martin ME, Meeks JC. (2007). Global gene expression patterns of *Nostoc punctiforme* in steady-state dinitrogen-grown heterocyst-containing cultures and at single time points during the differentiation of akinetes and hormogonia. *J Bacteriol* **189**: 5247–5256.
- Castenholz RW. (1988). Culturing methods for cyanobacteria. *Methods Enzymol* **167**: 68–93.
- Cordero OX, Polz MF. (2014). Explaining microbial genetic diversity in light of evolutionary ecology. *Nat Rev Microbiol* **12**: 263–273.
- Dagan T, Roettger M, Stucken K, Landan G, Koch R, Major P *et al.* (2013). Genomes of Stigonematalean cyanobacteria (Subsection V) and the evolution of oxygenic photosynthesis from prokaryotes to plastids. *Genome Biol Evol* **5**: 31–44.
- Dutta R, Inouye M. (2000). GHKL, an emergent ATPase/kinase superfamily. *Trends Biochem Sci* **25**: 24–28.
- Ehira S, Ohmori M, Sato N. (2003). Genome-wide expression analysis of the responses to nitrogen deprivation in the heterocyst-forming cyanobacterium *Anabaena* sp. strain PCC 7120. *DNA Res* **10**: 97–113.
- Ehlers A, Worm B, Reusch T. (2008). Importance of genetic diversity in eelgrass *Zostera marina* for its resilience to global warming. *Mar Ecol Prog Ser* **355**: 1–7.
- Flaherty BL, van Nieuwerburgh FV, Head SR, Golden JW, van Nieuwerburgh F. (2011). Directional RNA deep sequencing sheds new light on the transcriptional response of *Anabaena* sp. strain PCC 7120 to combined-nitrogen deprivation. *BMC Genomics* **12**: 332.
- Galperin MY. (2010). Diversity of structure and function of response regulator output domains. *Curr Opin Microbiol* **13**: 150–159.
- Gao R, Stock AM. (2009). Biological insights from structures of two-component proteins. *Annu Rev Microbiol* **63**: 133–154.
- Hedrick PW. (2006). Genetic polymorphism in heterogeneous environments: the age of genomics. *Annu Rev Ecol Evol. Syst.* **37**: 67–93.
- Hottes AK, Freddolino PL, Khare A, Donnell ZN, Liu JC, Tavazoie S. (2013). Bacterial adaptation through loss of function. *PLoS Genet* **9**: e1003617.
- Hughes JB, Daily GC, Ehrlich PR. (1997). Population diversity: its extent and extinction. *Science* **278**: 689–692.
- Huson DH, Bryant D. (2006). Application of phylogenetic networks in evolutionary studies. *Mol Biol Evol* **23**: 254–267.
- Kumar K, Mella-Herrera RA, Golden JW. (2010). Cyanobacterial heterocysts. *Cold Spring Harb Perspect Biol* **2**: a000315.
- Librado P, Rozas J. (2009). DnaSP v5: a software for comprehensive analysis of DNA polymorphism data. *Bioinformatics* **25**: 1451–1452.
- Luck GW, Daily GC, Ehrlich PR. (2003). Population diversity and ecosystem services. *Trends Ecol Evol* **18**: 331–336.
- Miller SR, Wingard CE, Castenholz RW. (1998). Effects of visible light and UV radiation on photosynthesis in a population of a hot spring cyanobacterium, a *Synechococcus* sp., subjected to high-temperature stress. *Appl Environ Microbiol* **64**: 3893–3899.
- Miller SR, Purugganan MD, Curtis SE. (2006). Molecular population genetics and phenotypic diversification of two populations of the thermophilic cyanobacterium *Mastigocladus laminosus*. *Appl Environ Microbiol* **72**: 2793–2800.
- Miller SR, Williams C, Strong AL, Carvey D. (2009). Ecological specialization in a spatially structured population of the thermophilic cyanobacterium *Mastigocladus laminosus*. *Appl Environ Microbiol* **75**: 729–734.
- Nakagawa S, Schielzeth H. (2013). A general and simple method for obtaining from generalized linear mixed-effects models. *Methods Ecol Evol* **4**: 133–142.
- Nei M. (1982). Evolution of human races at gene level. In: Bonne-Tamir B (ed). *Human Genetics, Part A: The Unfolding Genome*. Alan R Liss Inc.: New York, NY, USA, pp 167–181.
- Nicolaisen K, Hahn A, Schlieff E. (2009). The cell wall in heterocyst formation by *Anabaena* sp. PCC 7120. *J Basic Microbiol* **49**: 5–24.
- Oh H-M, Maeng J, Rhee G-Y. (1991). Nitrogen and carbon fixation by *Anabaena* sp. isolated from a rice paddy and grown under P and light limitations. *J Appl Phycol* **3**: 335–343.
- Phillips P. (2005). Testing hypotheses regarding the genetics of adaptation. *Genetica* **123**: 15–24.
- Reusch TBH, Ehlers A, Hammerli A, Worm B. (2005). Ecosystem recovery after climatic extremes enhanced by genotypic diversity. *Proc Natl Acad Sci USA* **102**: 2826–2831.
- Rodriguez-Valera F, Martin-Cuadrado A, Rodriguez-Brito B, Pašić L, Thingstad TF, Rohwer F *et al.* (2009). Explaining microbial population genomics through phage predation. *Nat Rev Microbiol* **7**: 828–836.
- Rosen MJ, Davison M, Bhaya D, Fisher DS. (2015). Fine-scale diversity and extensive recombination in a quasisexual bacterial population occupying a broad niche. *Science* **348**: 1019–1023.
- Rubio LM, Ludden PW. (2008). Biosynthesis of the iron-molybdenum cofactor of nitrogenase. *Annu Rev Microbiol* **62**: 93–111.
- Shapiro BJ, Friedman J, Cordero OX, Preheim SP, Timberlake SC, Szabo G *et al.* (2012). Population genomics of early events in the ecological differentiation of bacteria. *Science* **336**: 48–51.
- Stewart WD. (1970). Nitrogen fixation by blue-green algae in Yellowstone thermal areas. *Phycologia* **9**: 261–268.
- Stewart WD, Fitzgerald GP, Burns RH. (1967). *In situ* studies on N₂ fixation using the acetylene reduction technique. *Proc Natl Acad Sci USA* **58**: 2071–2078.
- Stucken K, Ilhan J, Roettger M, Dagan T, Martin WF. (2012). Transformation and conjugal transfer of foreign genes into the filamentous multicellular cyanobacteria (Subsection V) *Fischerella* and *Chlorogloeopsis*. *Curr Microbiol* **65**: 552–560.
- Tajima F. (1989). Statistical method for testing the neutral mutation hypothesis by DNA polymorphism. *Genetics* **123**: 585–595.
- Wall CA, Koniges GJ, Miller SR. (2014). Divergence with gene flow in a population of thermophilic bacteria: a potential role for spatially varying selection. *Mol Ecol* **23**: 3371–3383.
- Wolk CP. (2000). Heterocyst formation in *Anabaena*. In: Brun Y, Shimkets LJ (eds). *Prokaryotic Development*. ASM Press: Washington, DC, USA, pp 83–104.
- Zerbino DR, Birney E. (2008). Velvet: Algorithms for *de novo* short read assembly using de Bruijn graphs. *Genome Res* **18**: 821–829.

Supplementary Information accompanies this paper on The ISME Journal website (<http://www.nature.com/ismej>)